APPLIED AND ENVIRONMENTAL MICROBIOLOGY, Dec. 1996, p. 4632–4640 Vol. 62, No. 12
0099-2240/96/$04.00+0

Activity and Three-Dimensional Distribution of Toluene-Degrading *Pseudomonas putida* in a Multispecies Biofilm Assessed by Quantitative In Situ Hybridization and Scanning Confocal Laser Microscopy

SØREN MØLLER,[1] ANNE R. PEDERSEN,[2] LARS K. POULSEN,[3] ERIK ARVIN,[2] AND SØREN MOLIN[1]*

Department of Microbiology[1] and Institute of Environmental Science and Engineering,[2] The Technical University of Denmark, Lyngby, and BioImage, NOVO Nordisk,[3] Søborg, Denmark

Received 14 May 1996/Accepted 14 August 1996

As a representative member of the toluene-degrading population in a biofilter for waste gas treatment, *Pseudomonas putida* was investigated with a 16S rRNA targeting probe. The three-dimensional distribution of *P. putida* was visualized in the biofilm matrix by scanning confocal laser microscopy, demonstrating that *P. putida* was present throughout the biofilm. Acridine orange staining revealed a very heterogeneous structure of the fully hydrated biofilm, with cell-free channels extending from the surface into the biofilm. This indicated that toluene may penetrate to deeper layers of the biofilm, and consequently *P. putida* may be actively degrading toluene in all regions of the biofilm. Furthermore, measurements of growth rate-related parameters for *P. putida* showed reduced rRNA content and cell size (relative to that in a batch culture), indicating that the *P. putida* population was not degrading toluene at a maximal rate in the biofilm environment. Assuming that the rRNA content reflected the cellular activity, a lower toluene degradation rate for *P. putida* present in the biofilm could be estimated. This calculation indicated that *P. putida* was responsible for a significant part (65%) of the toluene degraded by the entire community.

The control and understanding of processes catalyzed by biofilms are important from an industrial as well as an ecological perspective, and this importance has motivated attempts to model biofilm growth and reaction kinetics mathematically. Most models envision biofilms as uniform structures, where active bacteria are randomly distributed in the biofilm matrix (17, 38). However, advances in nondestructive methods of microscopic analysis using scanning confocal laser microscopy (SCLM) (9, 23) have led to a more detailed picture, where biofilms consist of cell aggregates or microcolonies embedded in exopolysaccharide matrices. Microcolonies are interspersed with voids and water channels, making the biofilm heterogeneous (11). Liquid flow in such channels has been demonstrated (41), indicating that molecular diffusion is not the only process governing mass transport in biofilms. In fact, DeBeer et al. (12) showed that the channels can supply as much as 50% of the oxygen consumed by the biofilm.

In order to better understand the structure-function relationship in microbial biofilms, information about activity and spatial distribution of different subpopulations in biofilms is necessary. Applications of fluorescently labeled rRNA targeting probes have allowed identification of taxonomic groups of bacteria in multispecies biofilms (3, 36). However, the spatial distribution of the active bacteria in multispecies biofilms has been described in only a few cases. In a detailed study, the sulfate-reducing bacteria (SRB) of a trickling filter biofilm were investigated (35) by in situ hybridization in combination with O_2 and H_2S microelectrodes. The SRB population was shown to be predominant in the anoxic zone. Furthermore, the distribution of the major groups of gram-negative bacteria and a subpopulation of filamentous gram-negative bacteria has been visualized in activated sludge flocs by SCLM and in situ hybridization (44, 45).

The physiological activity and the growth rates of organisms present in multispecies biofilms are also poorly investigated. In a study by Poulsen et al. (33) using in situ hybridization coupled with image analysis, the SRB population of a multispecies biofilm grew faster in young biofilms than in an old, established biofilm community. Korber et al. (20) used cell elongation after addition of an inhibitor of DNA gyrase as an indicator of growth rate for *Pseudomonas fluorescens* in a monoculture biofilm. They found that cells at the biofilm-liquid interface elongated significantly more than cells located close to the substratum, indicating faster growth rates for cells close to the biofilm-liquid interface. Furthermore, cells at the biofilm-liquid interface have a higher energy charge than cells close to the substratum (19), also indicating a stratification in activity within the biofilm.

In the present analysis, we have used specific 16S rRNA probes to obtain information about the toluene-degrading population in a multispecies microbial consortium from a laboratory-scale biological filter for waste gas treatment. We have chosen a simplified approach in a first attempt to describe the toluene-degrading population from the biofilm community. A single toluene-degrading species was isolated from the community, and this isolate was investigated as a representative of the toluene-degrading population. Therefore, the validity of our predictions is based on the assumptions that this model organism is present in the community, that it participates in toluene degradation by performing at least some of the initial (rate-limiting) steps in the toluene degradation pathway in situ, and that it is responsible for a significant part of toluene removal by the community. In this framework, two features expected to be important in subsequent mathematical modeling of the system were investigated: (i) the spatial location of toluene degraders in the biofilm and (ii) the rate of toluene removal accomplished by this toluene-degrading subpopulation in the biofilm.

* Corresponding author. Mailing address: Department of Microbiology, Building 301, The Technical University of Denmark, DK-2800 Lyngby, Denmark. Phone: 45 45 25 25 13. Fax: 45 45 88 73 28. Electronic mail address: sm@im.dtu.dk.

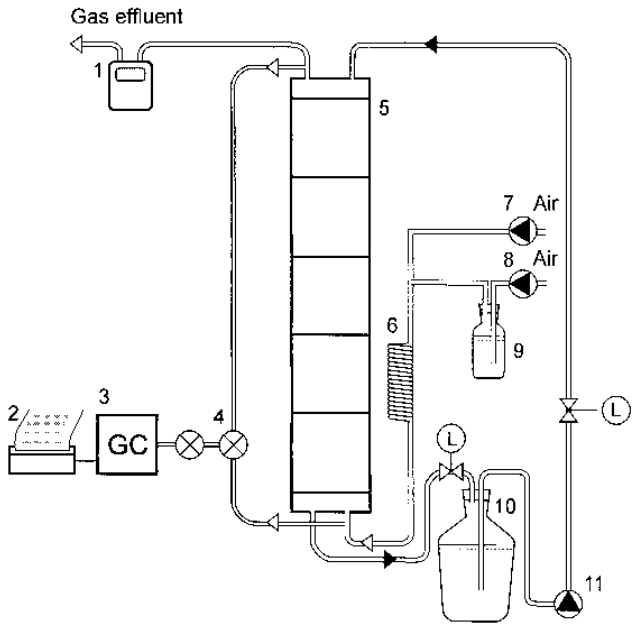

FIG. 1. Experimental setup. 1, gas flow meter; 2, integrator (Shimadzu C-R3A Chromatopac); 3, gas chromatograph (Shimadzu GC-14A); 4, two-points valve and eight-points valve for gas sampling; 5, filter column; 6, mixing coil; 7, membrane pump for air supply; 8, peristaltic pump; 9, pure toluene flask; 10, liquid container; 11, recirculation pump. L, sampling point for liquid.

MATERIALS AND METHODS

Design of the waste gas biofilter. The filter column was composed of stainless steel (Fig. 1) and consisted of five separated compartments in a stacked configuration (a total column height of 1.27 m). In each compartment was placed a polyvinyl difluoride cube (Mellapak 250; Sulzer Brothers Ltd., Winterthur, Switzerland) providing in total 4.83 m^2 of surface for biofilm growth (5.44 m^2, including the wall of the container). Each cube could be removed for biofilm sampling. The specific surface area was 250 $m^2\ m^{-3}$. Liquid was collected in the bottom of the column in a 5-liter container and recycled by addition to the top of the column (0.12 $m^3\ h^{-1}$), where it was distributed over the packing material through a plate with holes (5 mm in diameter and spaced by 20 mm). The toluene gas was produced by passing air through pure toluene and afterwards mixing the air-toluene mixture with the major airflow before entering the column at the bottom. This provided a countercurrent operation. The gas effluent was cooled to prevent the liquid from escaping from the column. A gas flow meter was placed at the gas effluent.

Inoculation and operation of the biofilter. The column was inoculated with a multispecies culture originating from a creosote-polluted aquifer (Fredensborg, Denmark). The starter culture was obtained from a previous experiment in which a trickling filter treating toluene was studied (31). Samples of the multispecies biofilm from the trickling filter were kept at −80°C. A sample was enriched on toluene (4 g m^{-3}) in batch culture before inoculation of the column. The inoculation was done in the water-filled column (with recirculation of the liquid), and after one day of starvation toluene (4 g m^{-3}) was added. After one more day of recirculation, the column was emptied and toluene was supplied in the gas flow. The filter was operated in the following way. Five liters of liquid was recirculated in the system and was renewed every three or four days. This liquid consisted of sterile tap water supplemented with nutrients at the following concentrations (in milligrams per liter): $NaNO_3$, 85; $Na_2HPO_4 \cdot 12H_2O$, 23; KH_2PO_4, 13; $FeSO_4 \cdot 7H_2O$, 6; EDTA, 1.1; (in micrograms per liter): $MnSO_4 \cdot H_2O$, 93; $Co(NO_3)_2 \cdot 6H_2O$, 160; $Na_2BO_7 \cdot 10H_2O$, 53; $Zn(NO_3)_2 \cdot 6H_2O$, 146; $Na_2MoO_4 \cdot 2H_2O$, 133; $NiSO_4 \cdot 7H_2O$, 77; KI, 20; $CuSO_4 \cdot 7H_2O$, 138. Furthermore, a nutrient solution was continuously added and contained the following components (in milligrams per day): $NaNO_3$, 1,300; $Na_2HPO_4 \cdot 12H_2O$, 345; KH_2PO_4, 195; $FeSO_4 \cdot 7H_2O$, 90; $MnSO_4 \cdot H_2O$, 1.4; $Co(NO_3)_2 \cdot 6H_2O$, 2.4; $Na_2B_4O_7 \cdot 10H_2O$, 0.8; $Zn(NO_3)_2 \cdot 6H_2O$, 2.5; $Na_2MoO_4 \cdot 2H_2O$, 2.0; $NiSO_4 \cdot 7H_2O$, 1.2; KI, 0.3; EDTA, 17; $CuSO_4 \cdot 7H_2O$, 2.1. The pH in the liquid was 8.2 ± 0.1, and the temperature was 24 to 26°C. Toluene was constantly fed to the column at 30 g $m^{-3}\ h^{-1}$, with a volumetric gas flow of (0.287 ± 0.002) $m^3\ h^{-1}$ and an inlet gas concentration of (2.0 ± 0.1) g m^{-3}. In order to obtain a constant liquid concentration through the column, the water was recirculated with a high volumetric flow ([0.11 ± 0.01] $m^3\ h^{-1}$).

Analytical techniques. Toluene in the liquid from the column was analyzed with a gas chromatograph (GC-9A; Shimadzu, Kyoto, Japan) equipped with a J & W Scientific column (DB1, 28 m) (catalog number 125-1032, series 9416145; J & W Scientific, Folsom, Calif.). The detector was a flame ionization detector connected to a computing integrator (C-R3A Chromatopac; Shimadzu). The analysis was carried out isothermally at 50°C. Liquid samples were collected in 10-ml volumetric flasks, and extraction was conducted by adding 500 μl of pentane containing heptane as an internal standard. One microliter of the pentane phase was injected into the gas chromatograph, and the ratios of the toluene and heptane responses were compared with standards. A Shimadzu gas chromatograph (GC-14 A) equipped with an on-line injection system was used for analysis of toluene in the gas phase. The gas chromatograph was supplied with a packed column of stainless steel containing 80/120 Carbopack B (3% SP-1500 packing) (Supelco Inc., Bellefonte, Pa.). The on-line injection system consisted of a two-points valve (Valco Instruments Co. Inc., Schenkon, Switzerland) with a sample loop of 1.0 ml and an eight-points valve to select the sampling point. The eight-points valve was connected to the gas inlet and the gas effluent from the column by stainless steel tubes. Gas samples were loaded by a peristaltic pump at the outlet of the two-points valve with a flow rate of 10 ml min^{-1}. On-line injection was conducted automatically and carried out isothermally at 180°C. A flame ionization detector was used, and the responses were collected by a computing integrator (C-R5A Chromatopac; Shimadzu). Gas standards of defined concentrations were made for calibration.

Isolation and characterization of toluene degraders. Samples from the community were repeatedly plated on LB medium (4). Selected isolates with a distinct colony morphology were isolated and tested for toluene degradation in the following way. Isolates were inoculated into 50 ml of medium with toluene (4 g m^{-3}). The flasks were closed with Mininert valves (Dynatech Precision Sampling Corp., Baton Rouge, La.) and incubated at 25°C. Toluene degradation was measured by withdrawing 1 μl of the liquid phase, and the toluene concentration was determined by gas chromatographic analysis as described above (Analytical techniques). The data were compared with those from a sterile control. The isolate with the highest toluene degradation rate was closely related to *Pseudomonas putida* (see below) and was named *P. putida* R1.

The potential for toluene degradation of the *P. putida* population was tested by plating samples from the community on rich media and isolating autofluorescent colonies (when illuminated with UV light). These were taken to be indicative of fluorescent pseudomonads. Sixteen individual colonies were isolated and tested for the ability to grow on AB minimal media (10) either with toluene supplied as vapor or with 5 mM benzyl alcohol. The Biolog test was performed according to the manufacturer's recommendations, and isolates were identified with ML release 3.50 (Biolog, Hayward, Calif.). For testing of probe specificity, all isolates were grown exponentially in LB medium (4).

Degradation kinetics of *P. putida* R1. The toluene degradation kinetics of *P. putida* R1 were examined in batch culture at 25°C with toluene (3 g m^{-3}) as the sole carbon source. Toluene removal was monitored by measuring the toluene concentration on-line in a liquid loop (22) with a membrane inlet mass spectrometer (TCP-121; Balzers AG, Balzers, Fürstentum Liechtenstein). The liquid in the batch system was passed through a cell with a silicone-rubber membrane separating the liquid from the vacuum chamber of the mass spectrometer. The mass spectrometer was equipped with a quadruple analyzer and a Faraday cup detector. The software Quadstar 421 (Balzers AG) was used for collecting the data and for quantitative analysis. Calibration was made with standards controlled by the gas chromatograph. Development of biomass in the system was measured as protein in 10-ml liquid samples withdrawn by adding air through a sterile filter. Toluene and protein concentrations were fitted to a Monod model (7), and the kinetic parameters were estimated (see Table 4).

Sampling of biofilm. The biofilm thickness was measured by the weight of the total amount of biomass on one cube using a biofilm density of 1 g cm^{-3} and the total surface area of one cube (0.967 m^2). The biofilm was sampled by scraping of a known area (6 to 20 cm^2) of biofilm, which was transferred to Milli-Q water (Millipore Corp., Bedford, Mass.). Samples were disintegrated with a sonicator (Branson Sonifier; Branson Ultrasonics Corp., Danbury, Conn.) for 4 min at an output control of setting 2 and a duty cycle of 50%. The protein content of the biofilm was determined by the method of Lowry et al. (25) with bovine serum albumin (Sigma Chemical Company, St. Louis, Mo.) as the standard. Before analysis, cells were lysed with 0.5 M trichloroacetic acid. Biofilm polymer was determined by a colorimetric method (14) using glucose as a standard.

For quantitative hybridizations, disintegrated samples were fixed in 3% paraformaldehyde. For the structural analysis, intact biofilm samples for hybridization were collected from the column on small 8- by-40-mm plastic strips (pieces of a regular plastic folder) (BIPC; Barfod & I. Chr. Petersen a/s, Glostrup, Denmark) mounted on a coverslip (10 by 50 mm). This support was found to be practically nonfluorescent and hence ideal for subsequent hybridization. Coverslips with plastic pieces were glued onto the polyvinyl difluoride cubes and placed in the column before inoculation. Biofilm samples were fixed in 3% paraformaldehyde, washed in phosphate-buffered saline, dehydrated as previously described (29), and then stored at −20°C.

Sequencing of 16S rRNA. Sequencing of 16S rRNA was performed with an automatic 373A DNA Sequencer (Applied Biosystems, Foster City, Calif.) directly on PCR products generated from chromosomal DNA extracts according to the manufacturer's recommendations. The following primers, optimized for pseudomonads, were used (in the 5′-to-3′ direction): 11F, GTTTGATC(A/C)TGGC TCAGATTG; 344R, CCCCACTGCTGCCTCCCGT; 515R, GTATTACCGCG

GC(G/T)GCTGGCAC; 922R, GCTTGTGCGGGCCCCCGTC; 1101R, GACA AGGGTTGCGCTCGTT; 1389R, GTGACGGGCGGTGTGTACAAG; and 1465R, CCCCAGTCATGAATCATAAAGTGGT. F indicates forward and R indicates reverse. The isolate from the column with the highest specific toluene degradation rate was closely related to *P. putida* as inferred from the 16S rRNA sequence with the PHYLIP software (15).

Oligonucleotide probes. For hybridizations, the probe EUB338, specific for the domain *Bacteria* (1), and a probe specific for the *P. putida* 16S rRNA (PP986; 5′-TCTCTGCATGTCAAGGCCT-3′) were used. Initially, the specificity of PP986 was tested against published sequences with the CHECK_PROBE program from the ribosomal database project (26). Oligonucleotide probes were synthesized with an automatic DNA synthesizer, and an aminohexyl linker (Aminolink 2; Applied Biosystems) was attached at the 5′ terminus by use of a standard DNA synthesis cycle. The probes were labeled with the isothiocyanate derivative CY3 or CY5 (Biological Detection Systems, Pittsburgh, Pa.) and purified by fast protein liquid chromatography as previously described (34). Furthermore, probes were labeled with fluorescein at the 5′ end during the synthesis of the oligonucleotide with fluorescein–*N*,*N*-diisopropyl-β-cyanoethyl phosphoramidite (Peninsula Laboratories, Inc., Belmont, Calif.).

Hybridization of whole cells. For quantitative hybridization of disintegrated biofilm samples, cell smears were applied to poly-L-lysine (Sigma Chemicals, St. Louis, Mo.)-coated slides (slides were cleaned in 1% HCl in 70% ethanol, dipped into 0.01% poly-L-lysine solution, and air dried) and dehydrated by sequential washes in 50, 80, and 96% ethanol (3 min each). After the samples were washed with ethanol, 10 μl of hybridization mixture (30% formamide, 0.9 M NaCl, 100 mM Tris [pH 7.2], 0.1% sodium dodecyl sulfate) containing 25 ng of the probe was added to each hybridization well. Cells were incubated with hybridization solution for 16 h at 37°C in a moisture chamber. For washing, the slides were submerged in 100 ml of washing solutions. First the slides were washed in washing solution I (30% formamide, 0.9 M NaCl, 100 mM Tris [pH 7.2], 0.1% sodium dodecyl sulfate) for 20 min at 37°C, then they were transferred to a DAPI (4′,6-diamidino-2-phenylindole) staining solution (0.1 M Tris [pH 7.2], 0.9 M NaCl, 6.25 μM DAPI) for 3 min at 21°C, subsequently they were washed for 15 min in washing solution II (0.1 M Tris [pH 7.2], 0.9 M NaCl) at 37°C, and finally they were rinsed in 100 ml of distilled water. Intact biofilm samples were hybridized in the following way. A small piece of the plastic support with biofilm was cut from the coverslip with a scalpel and glued to a Teflon-coated slide with regular nail polish. Subsequently, the biofilm samples were hybridized as cell smears except that the washing steps were longer: 1 h and 1.5 h in washing solutions I and II, respectively.

Acridine orange staining. To preserve biofilm structure, biofilm samples from the reactor were embedded in 0.7% agarose (Sigma, St. Louis, Mo.) as suggested by Massol-Deyá et al. (28), fixed in 3% paraformaldehyde, and stored in 1× phosphate-buffered saline at 4°C. Staining with acridine orange (AO) was performed directly on a piece of biofilm cut out of the agar by placement of the sample in a petri dish in 10 ml of AO staining buffer (22 μM AO, 5 mM EDTA, 0.15 M NaCl, 0.1 M phosphate-citrate buffer [pH 6]) as described previously (29). However, no washing step was performed.

Epifluorescence microscopy. Hybridized samples were analyzed by the use of a Carl Zeiss Axioplan epifluorescence microscope. The excitation source was a 100-W HBO bulb, and digital images were captured with a 12-bit cooled slow-scan charge-coupled device (CCD) camera (KAF 1400 chip; Photometrics, Tucson, Ariz.). The CCD camera was controlled by PMIS software (Photometrics). For quantitative hybridizations, CY3-labeled probes were used. CCD exposure times of 2 s were used, and the cells were counterstained with DAPI and EUB338 labeled with fluorescein. Furthermore, the captured images for rRNA measurements were focused with the filter set 1 (Carl Zeiss) for DAPI to avoid bleaching of the CY3 fluorochrome. CY3-, CY5-, and fluorescein-labeled cells were visualized by the use of the filter sets XF40 (Omega Opticals, Brattleboro, Vt.), XF45 (Omega Opticals), and 10 (Carl Zeiss), respectively.

Image analysis. The amount of light from hybridized cells was quantified by use of the Cellstat image analysis program (29). For each analysis, the average intensity of three different images corresponding to between 30 to 150 cells was used. Cellstat is a UNIX-based image analysis program capable of handling 16-bit image data. The basis for the Cellstat object recognition are cell size (area, in pixels) and various shape parameters. On-line information is available on the World Wide Web at URL http://www.im.dtu.dk/cellstat/index.html.

Counting of *P. putida* in biofilm samples. One-microliter aliquots of disintegrated biofilm samples were applied to a poly-L-lysine-coated slide, and hybridization was performed as described above. In seven randomly chosen microscopic fields, PP986- (CY3) and EUB338 (fluorescein)-stained cells were counted with appropriate filter sets. The sizes of fields were chosen such that the average was 20 to 30 cells per field, and statistics were calculated with the COUNT program from Bloem et al. (5). The utility of in situ hybridization in describing this multispecies community was confirmed by showing that between 75 and 95% of the DAPI-stained organisms also stained with the probe EUB338, specific for the domain *Bacteria* (data not shown). This indicates that most bacteria could be detected by whole-cell hybridization, and the proportion detectable is similar to that found in other natural communities (46).

SCLM. A Carl Zeiss confocal laser microscope (LSM 410; Carl Zeiss, Oberkochen, Germany) was used to obtain optical thin sections of the biofilm. *P. putida* and members of the domain *Bacteria* were visualized simultaneously by hybridizing the biofilm with CY3-labeled PP986 and CY5-labeled EUB338. Dual excitation was obtained by using the 633-nm line (for CY5) and the 543-nm line (for CY3) of a helium-neon laser. Lasers were operated at 1/10 maximum strength, and the pinhole was set to 17. Images were optimized by adjusting the brightness and contrast settings. Simultaneous sampling of the two fluorochromes was achieved with an NT 80/20 filter (Carl Zeiss). For visualization of AO-stained biofilm, the setting for CY3 was used (excitation filter LP 515). A ×63 Apochromat (numerical aperture, 1.4; Carl Zeiss) was used in all experiments. Images were processed with Photoshop (Adobe, Mountain View, Calif.), and three-dimensional space-filling reconstructions were made with Spyglass Slicer (Spyglass Inc., Champaign, Ill.).

Calculation of in situ toluene degradation kinetics. Based on the high affinity of *P. putida* R1 for toluene (half saturation constant [K_s] = 0.1 mg liter^{-1}) the maximal toluene degradation by *P. putida* in the biofilm was described by assuming a zero-order reaction using the following equation:

$$r_{a,putida(max)} = k_{m,putida} X_{a,putida} \quad (1)$$

$r_{a,putida(max)}$ is the maximal surface removal rate of toluene (in grams per square meter per day) (g_s m^{-2} d^{-1}). $X_{a,putida}$ is the concentration of active biomass of *P. putida* per unit surface area of the biofilm (in grams per square meter) (g_x m^{-2}), and $k_{m,putida}$ is the maximal specific substrate degradation rate (g_s g_x d^{-1}) measured in a batch experiment. By using cellular rRNA levels as an indication of in situ activity, $k_{m,putida}$ is reduced by a factor *R*, called the correction factor for metabolic activity in situ. This gives the following equation for estimating toluene degradation kinetics for *P. putida* in the biofilm:

$$r_{a,putida} = R\, k_{m,putida} X_{a,putida} \quad (2)$$

R was estimated for toluene-degrading *P. putida* in the biofilm by comparing the measured rRNA content with a standard curve correlating growth rate and rRNA content for *P. putida* KT2442. The correlation between rRNA content and growth rate was found to be similar for the two *P. putida* isolates (29a). The regression line obtained for *P. putida* KT2442 was $C = 1.05\mu + 0.193$ (29), where μ is the growth rate and *C* is the rRNA content measured relative to the rRNA content at maximum growth rate. From a relative rRNA content measured in the biofilm an apparent μ can be calculated, which is then normalized to $\mu_{max} = 0.77$ h^{-1} (where $C = 1$) to give the correction factor for metabolic activity, *R*. The complete equation is then:

$$R = (C - 0.193)/0.81 \quad (3)$$

Nucleotide sequence accession number. The sequence reported here will appear in the EMBL, GenBank, and DDBJ nucleotide sequence databases under the accession number X93997.

RESULTS AND DISCUSSION

Design of a probe specific for toluene degraders. In the process of isolating an important toluene degrader from the multispecies biofilm community, numerous different colony morphologies were observed when samples from the community were cultured on plates. Various dominant isolates were tested for toluene degradation, and the degradation kinetics of several toluene degraders were determined (data not shown). The isolate with the highest specific toluene degradation rate was identified as *P. putida* by sequencing of the 16S rRNA gene, and the isolate was named *P. putida* R1. The 16S rRNA sequence was used by sequence comparison to design a *P. putida*-specific ribosomal probe, PP986, complementary to the region around base number 986 of the 16S rRNA (*E. coli* numbering [8]). PP986 was tested against published sequences and showed one or more mismatches to all species except *P. putida*. For further evaluation of probe specificity, PP986 was tested by whole-cell hybridization against a broad spectrum of bacteria and was apparently specific for the *P. putida* A subgroup (Table 1). A *P. putida*-specific probe has previously been designed that targets the 23S rRNA (40). However, this probe also targets *P. mendocina* (2). The probe PP986 targets *P. putida* biotype A and is therefore more specific.

The toluene degradation potential of the *P. putida* population in the biofilm was tested by isolating fluorescent pseudomonads from the community and testing these for toluene degradation. All isolates (16 individual clones) and *P. putida* R1 were able to grow with toluene as the sole carbon source,

TABLE 1. Test of specificity of the *P. putida* probe PP986 as assessed by whole-cell hybridization

Source	Strain	Phylogenetic affiliation	Hybridization[a]	
			EUB338	PP986
Isolated from the community	*Pseudomonas putida* R1	γ-Proteobacteria	+	+
—[b]	*Pseudomonas putida* KT2442	γ-Proteobacteria	+	+
ON27[c]	*Pseudomonas putida* A	γ-Proteobacteria	+	+
ON34[c]	*Pseudomonas putida* A	γ-Proteobacteria	+	+
DSM50226	*Pseudomonas putida*	γ-Proteobacteria	+	+
DSM291	*Pseudomonas putida*	γ-Proteobacteria	+	+
DF45[c]	*Pseudomonas putida* B	γ-Proteobacteria	+	−
DF13[c]	*Pseudomonas putida* B	γ-Proteobacteria	+	−
—[d]	*Pseudomonas fluorescens* R2F	γ-Proteobacteria	+	−
DSM50090	*Pseudomonas fluorescens*	γ-Proteobacteria	+	−
DSM50148	*Pseudomonas fluorescens*	γ-Proteobacteria	+	−
DSM50106	*Pseudomonas fluorescens*	γ-Proteobacteria	+	−
ATCC 13525	*Pseudomonas fluorescens*	γ-Proteobacteria	+	−
DSM39	*Pseudomonas acidovorans*	γ-Proteobacteria	+	−
ATCC 10145	*Pseudomonas aeruginosa*	γ-Proteobacteria	+	−
LM2402-8	*Pseudomonas aeruginosa*	γ-Proteobacteria	+	−
ATCC 9447	*Pseudomonas chlororaphis*	γ-Proteobacteria	+	−
ATCC 43928	*Pseudomonas chlororaphis*	γ-Proteobacteria	+	−
ATCC 10857	*Pseudomonas chlororaphis*	γ-Proteobacteria	+	−
ATCC 13985	*Pseudomonas aureofaciens*	γ-Proteobacteria	+	−
DSM50227	*Pseudomonas stutzeri*	γ-Proteobacteria	+	−
ATCC 25411	*Pseudomonas mendocina*	γ-Proteobacteria	+	−
DSM1532	*Acinetobacter calcoaceticus*	γ-Proteobacteria	+	−
DSM590	*Acinetobacter calcoaceticus*	γ-Proteobacteria	+	−
Isolated from the community	*Acinetobacter* strain C6	γ-Proteobacteria	+	−
—[e]	*Enterobacter cloacae*	γ-Proteobacteria	+	−
—[f]	*Escherichia coli* BJ4	γ-Proteobacteria	+	−
—[g]	*Rhizobium meliloti*	α-Proteobacteria	+	−
DSM107	*Rhodospirillum rubrum*	α-Proteobacteria	+	−
—[g]	*Chromobacterium violaceum*	β-Proteobacteria	+	−
DSM50180	*Pseudomonas cepacia*	β-Proteobacteria	+	−
DSM416	*Alcaligenes eutrophus*	β-Proteobacteria	+	−
—[g]	*Bacillus subtillis*	Gram positive (low G+C)	+	−
—[g]	*Micrococcus luteus*	Gram positive (high G+C)	+	−

[a] +, positive reaction with PP986; −, no visible hybridization.
[b] From de Lorenzo et al. (13).
[c] From Ole Nybroe (42) at The Royal Veterinary and Agricultural University, Frederiksberg, Denmark.
[d] From van Overbeek et al. (43).
[e] From Pedersen and Jacobsen (32).
[f] From Krogfelt et al. (21).
[g] From the Department of Microbiology strain collection, The Technical University of Denmark.

and all hybridized with the probe PP986. By evaluation of Biolog substrate utilization patterns, the isolates were identified as *P. putida* type A1 with similarity indexes between 0.734 and 0.857. The probe PP986 was therefore highly specific for targeting toluene-degrading *P. putida* in this biofilm community.

By using the probe PP986 to enumerate the population of toluene-degrading *P. putida* in the steady-state bioreactor, the relative frequency of *P. putida* in the community was about 4% (Table 2). This shows that the strain of *P. putida*, which was isolated by simple plating and which had the highest toluene degradation rate of the different isolated species, was also present in the community as a significant subpopulation. We have previously developed methods for describing the physiological state of bacterial cells at the single-cell level by measuring growth rate-related parameters such as rRNA content and cell size with quantitative hybridizations coupled with image analysis (29). With this method, the average rRNA content of the *P. putida* population in the biofilm was found to be 65% ± 36% (mean ± coefficient of variation) of the rRNA content of a batch culture of strain R1 grown on toluene (Table 2). The cell volume was 95% ± 57% of exponentially grown *P. putida* R1 (Table 2). This further suggested that the *P. putida* population was quite active in the community, and we therefore chose *P. putida* as a model organism for the toluene-degrading population in the biofilm.

Biofilm architecture. The three-dimensional distribution of the *P. putida* population and the spatial heterogeneity of the biofilm were visualized by SCLM. Figure 2 shows optical thin sections of the hybridized biofilm at different depths, demonstrating the presence of *P. putida* at all depths in the biofilm. *P. putida* was present in dense cell clusters (microcolonies) and as individual cells distributed throughout the biofilm. In the optical section 20 μm from the biofilm surface, a dividing cell

TABLE 2. Data on *P. putida* in the biofilm

Parameter[a]	Value ± coefficient of variation
Relative no. of *P. putida* cells in biofilm	4%
Relative rRNA content	65 ± 36%
Relative cell vol	95 ± 57%

[a] Measured with PP986.

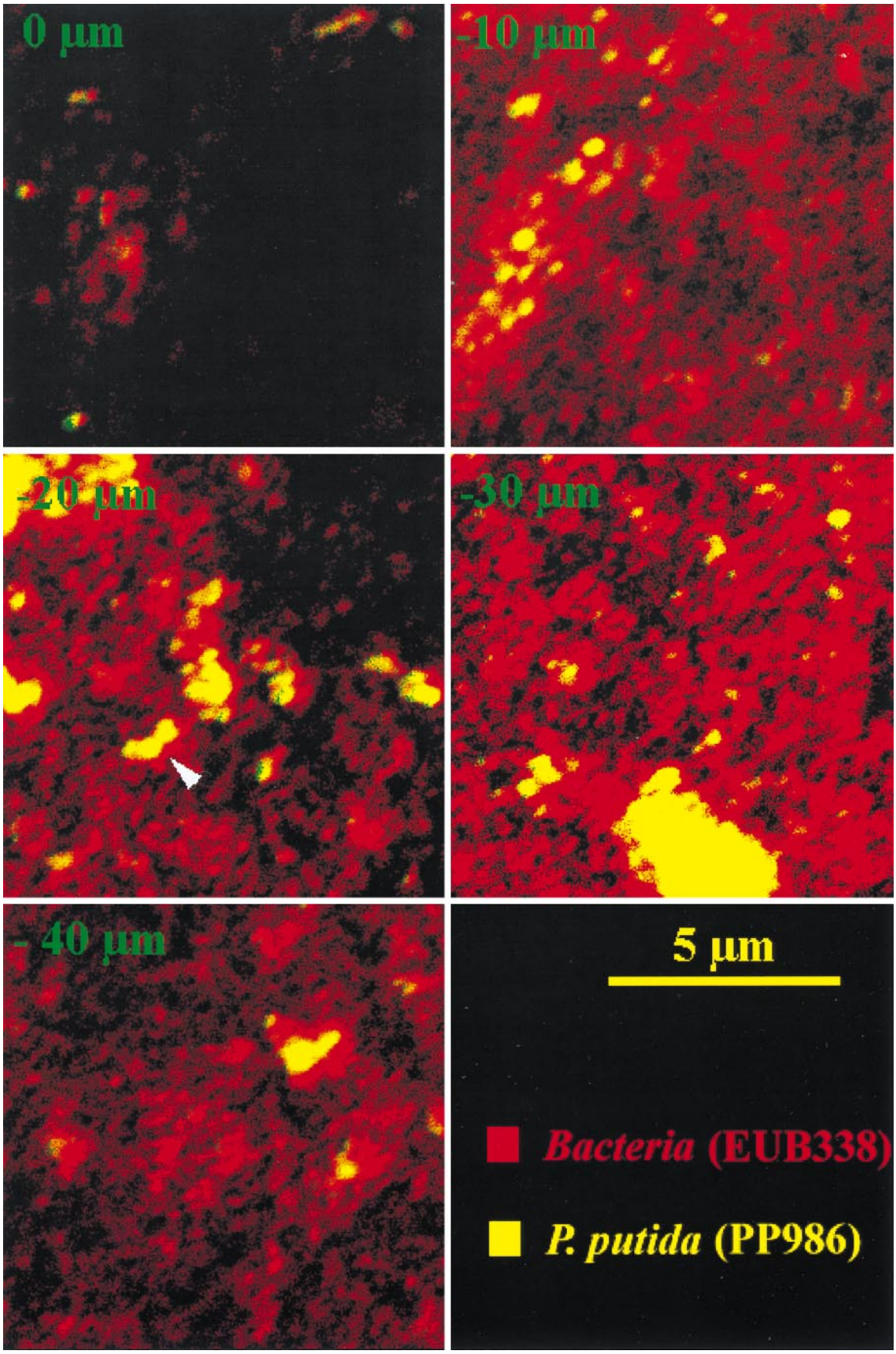

FIG. 2. Optical sectioning of the toluene-degrading biofilm visualizing the spatial distribution of *P. putida*. The biofilm was hybridized with CY3-labeled PP986 and CY5-labeled EUB388 to visualize *P. putida* and members of the domain *Bacteria* simultaneously. Optical thin sections at different depths of the biofilm are shown. 0 μm indicates the surface of the biofilm, whereas −10, −20, −30, and −40 μm indicate the distance from the surface. Optical sections were sampled with 1.0-μm increments, and each section represents a sum of three images. Cells stained with a probe for the domain *Bacteria* are sampled in the red channel and will appear red, whereas cells stained with the *P. putida* probe are sampled in the green channel. Since *P. putida* cells are targeted with both EUB338 and PP986, such cells are sampled in both channels and will appear yellow.

was observed (see arrow in Fig. 2), indicating an actively growing population. By generating space-filling reconstructions, the three-dimensional localization of *P. putida* in the biofilm matrix could be visualized (Fig. 3). This clearly documents the presence of *P. putida* as single cells and dense cell clusters throughout the vertical dimension of the biofilm.

The hybridization protocol includes a dehydration step, which causes collapse of the biofilm structure. To give an indication of the degree of dehydration, the average thickness of the fully hydrated biofilm was 356 μm (Table 3), compared with thicknesses between 25 and 70 μm when the dehydrated biofilms were observed by SCLM. To investigate the structure of the fully hydrated biofilm, samples of the biofilm were embedded in agarose and positively stained with AO. Figure 4A shows optical sectioning of a fully hydrated biofilm stained with AO, and horizontal sections at different depths from the surface of the biofilm are shown. This visualizes the presence of cell-free volumes extending from the surface into deeper regions of the biofilm. Figure 4B shows a sagittal section visualizing channels extending from the surface into the biofilm, further indicating the heterogeneity of the biofilm structure.

A simple biofilm model based on diffusion-limited substrate transport in the biofilm would predict that toluene-degrading bacteria are located in the outermost layers of the biofilm, where the substrate concentration is the highest (37). Such a model does not seem to be sufficient to describe the three-

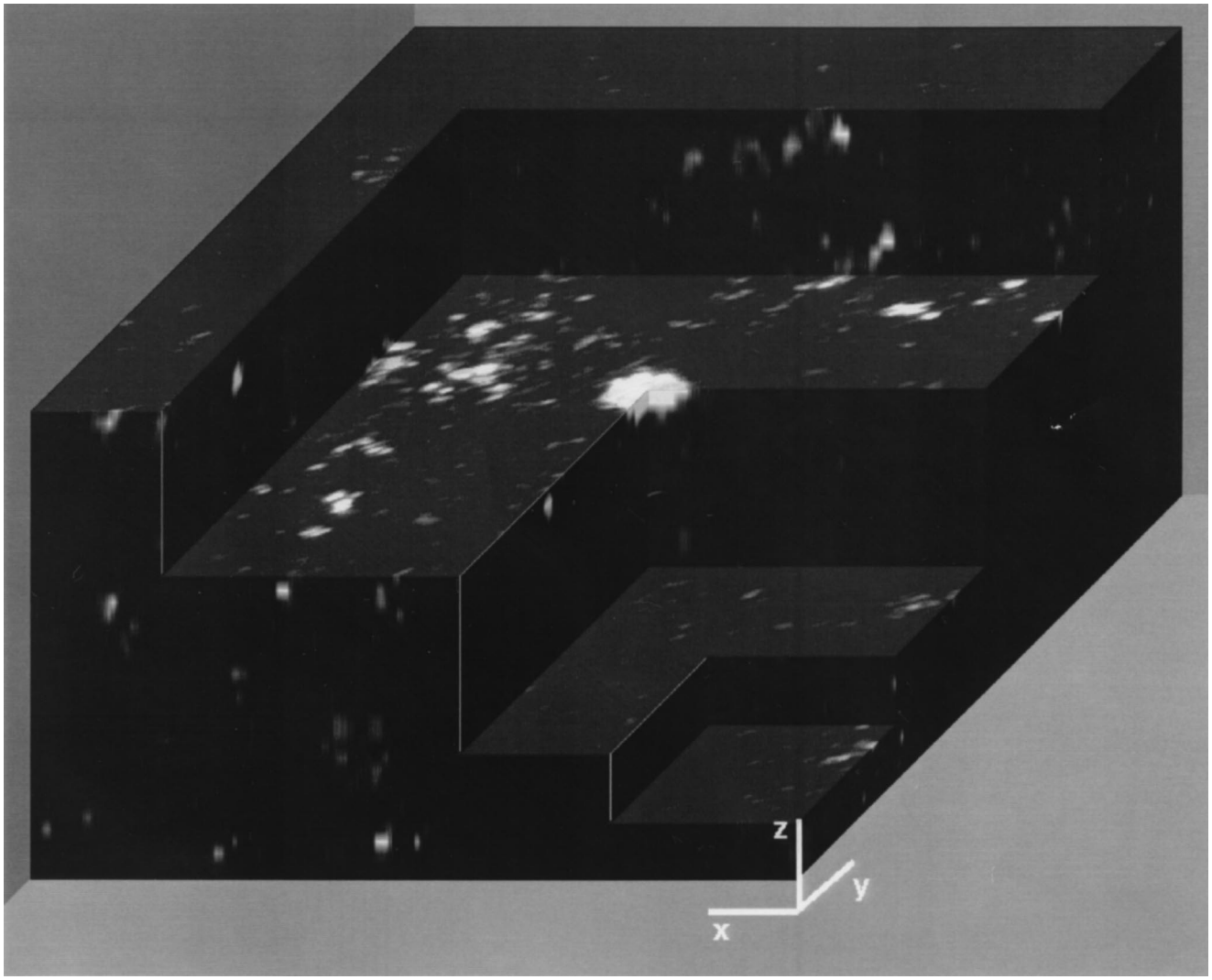

FIG. 3. Illustration of the three-dimensional distribution of toluene-degrading *P. putida* cells in the matrix of the multispecies biofilm. Only *P. putida* cells are shown as positively stained (white) cells, whereas members of the domain *Bacteria* are not visualized. The three-dimensional space-filling reconstruction was made from 40 individual optical sections sampled with 1-μm increments.

TABLE 3. Biofilm data at steady state

Parameter	Abbreviation for parameter	Value
Biofilm thickness	L	356 μm
Protein content	X_{prot}	3.23 g m^{-2}
Active biomass[a]	X_a	6.46 g m^{-2}
Polymer content	X_p	2.04 g m^{-2}
Toluene surface removal rate	r_a	2.30 g_s m^{-2} day^{-1}
Toluene load	L_d	30 g m^{-3} h^{-1}
% Toluene removal	E	80%

[a] The active biomass in the biofilm is estimated as two times the protein content.

dimensional location of toluene degraders in the biofilm developed in this waste gas biofilter. The porous biofilm structure observed here suggests that toluene could penetrate the biofilm to a higher degree than if the mass transport were governed by diffusion alone. Channel structures have been shown to facilitate substrate transport into biofilms (12, 23, 41), indicating that substrate may be available to the *P. putida* cells localized deep inside the biofilm, allowing them to degrade toluene.

Determination of the rate of toluene removal. In the biofilter, a quasi-steady state was obtained after about 1.5 months of operation. The data in Table 3 give the details of biofilm composition and reactor performance. An estimate of the contribution of the *P. putida* population to the total toluene degradation in the biofilm was calculated by combining the in situ hybridization data (Table 2) and the kinetic data (Table 4). Although the biofilm was quite heterogeneous, as was discussed above, there is no indication that toluene is metabolized only in specific parts of the community. In contrast, since the coefficient of variation (CV) of the rRNA content for the *P. putida* population (36% [Table 2]) is in the range of what has been found for chemostat cultures of *P. putida* KT2442, measured by hybridization and image analysis (from 20 to 30% [29]), it is likely that the physiological activity of the *P. putida* biofilm population was rather homogeneous. There are further indications that toluene degradation could be taking place in deeper regions of the biofilm. The *P. putida* cells in the biofilm contained significantly more rRNA than the heterotrophic population as judged by hybridization with the probe for the domain *Bacteria* (data not shown). This indicated that the *P. putida* cells located deep in the biofilm were more physiologically active than the surrounding bacteria, suggesting that *P. putida* had access to a substrate (toluene) not available to the heterotrophic population. Furthermore, all the fluorescent pseudomonads isolated from the system grew on benzyl alcohol (data not shown), which provided a very preliminary indication that the initial steps in the degradation of toluene were similar to the upper pathway of the TOL plasmid (27). This suggested that all of the *P. putida* cells in the biofilm were using the same degradative pathway, making the existence of a subpopulation of non-toluene-degrading *P. putida* unlikely. There-

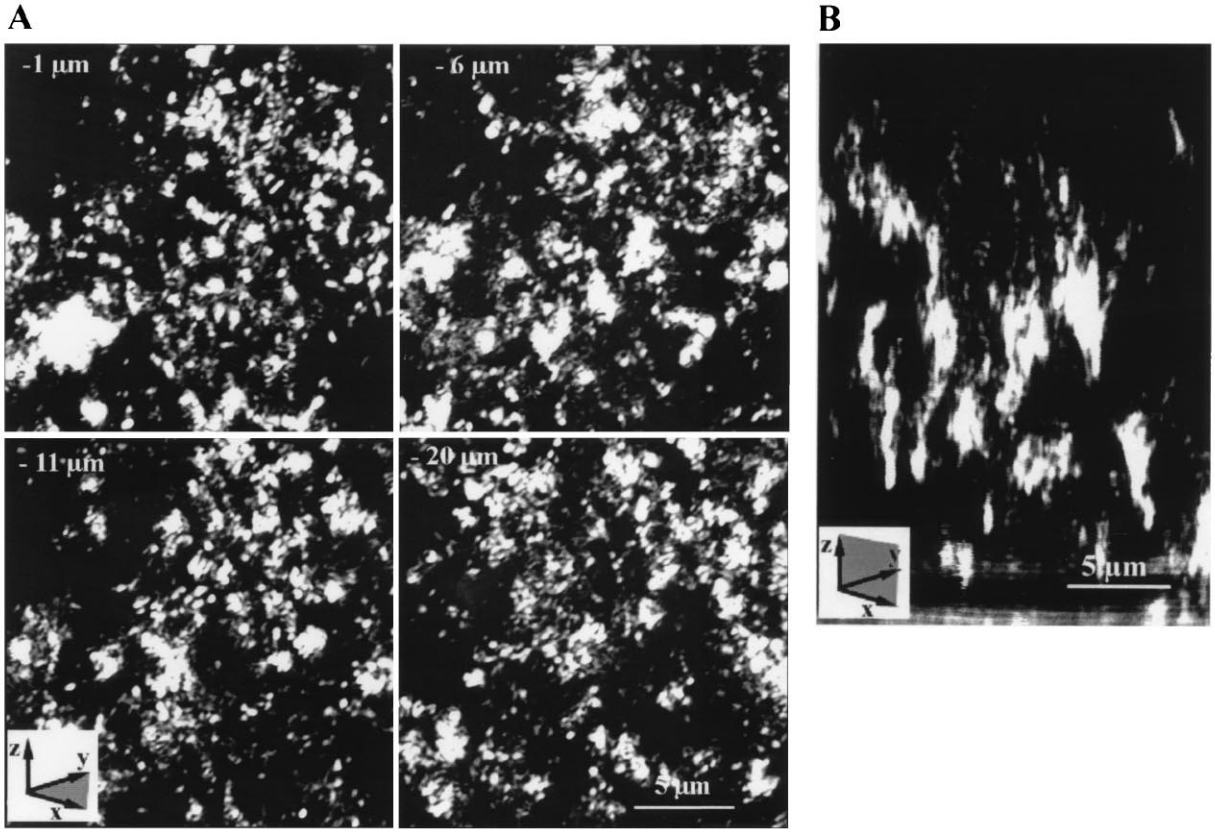

FIG. 4. Optical sectioning of a fully hydrated biofilm stained with AO to visualize the heterogeneous structure of the toluene-degrading biofilm. (A) Optical sections at different depths from the biofilm surface (0 μm). Optical sections were sampled with 0.4-μm increments, and each section represents a sum of three images. (B) Sagittal optical section. The biofilm was sampled from the column and embedded in 0.7% agarose to preserve the hydrated structure. See axis legend to identify the plane of image display.

TABLE 4. Kinetics of toluene degradation by *P. putida* in pure culture and in the biofilm

Parameter	Abbreviation for parameter	Value
Maximum specific toluene removal rate by *P. putida* in batch culture	$k_{m,putida}$	10.1 g_s $g_{xa,putida}^{-1}$ day^{-1}
P. putida biomass in the biofilm[a]	$X_{a,putida}$	258 mg_s m^{-2}
Maximum surface removal rate by *P. putida* in situ[b]	$r_{a,putida(max)}$	2.61 g_s m^{-2} day^{-1}
Correction factor for in situ metabolic activity[c]	R	0.57
Toluene surface removal rate by *P. putida* in situ[d]	$r_{a,putida}$	1.49 g_s m^{-2} day^{-1}

[a] $X_{a,putida}$ was calculated assuming that 4% of the total biomass (X_a) consisted of *P. putida*.
[b] $r_{a,putida(max)}$ was calculated by assuming that *P. putida* degrades toluene with the maximal rate in the biofilm using $r_{a,putida} = k_{m,putida} \times X_{a,putida}$ (equation 1).
[c] R was calculated from the rRNA content of *P. putida* measured in the biofilm (equation 3).
[d] $r_{a,putida}$ was calculated as $R \times k_{m,putida} \times X_{a,putida}$ (equation 2).

fore, the toluene degradation rate for the *P. putida* population was estimated as an average, ignoring spatial heterogeneity and using the kinetic data for the isolate R1. Assuming a zero-order reaction rate, the maximal surface removal rate for *P. putida* R1 was determined to be $r_{a,putida(max)} = 2.61$ g_s m^{-2} d^{-1} (Table 4). This maximal rate is 14% higher than the surface removal rate measured for the entire biofilm community ($r_a = 2.30$ g_s m^{-2} d^{-1}).

However, assuming a maximal zero-order degradation rate for *P. putida* (i.e., no substrate limitation in the biofilm) may overestimate the substrate removal rate of this population in the biofilm. The rRNA content and cell size of *P. putida* in the biofilm environment were reduced relative to those measured under optimal conditions for *P. putida* R1 grown in batch culture with toluene as the only carbon source (Table 2). The ribosome content of the bacterial cell is believed to be tightly regulated and coupled to the level of cellular activity, i.e., protein synthesis (18). The rate of protein synthesis, and hence the rRNA content, must depend on the flux of carbon available to the cell. Furthermore, the cellular rRNA content and growth rate have been demonstrated for many bacterial species to be proportional (6, 29, 30, 39), and basic chemostat equations show that the growth rate, under such conditions, is determined by the substrate concentration (16). Therefore, this altered physiological state could reflect a suboptimal toluene degradation rate in situ. The toluene degradation rate could be calculated, considering the reduced cellular activity, by correcting the maximal specific toluene removal rate ($k_{m,putida}$) with a factor R (the correction factor for the metabolic activity in situ). The factor R is taking the measured rRNA content into account (Materials and Methods, equation 3). For the *P. putida* population present in the biofilm, R was 0.57 (Table 4), giving an estimated surface removal rate of *P. putida* in the biofilm of $r_{a,putida} = 1.49$ g_s m^{-2} d^{-1}. This constituted about 65% of the toluene degradation rate of the entire biofilm. The calculation illustrated how a toluene-degrading population constituting only 4% of the total population may be sufficient to account for most of the toluene removal performed by the entire biofilm community and suggested that *P. putida* may be a major toluene degrader in the community.

The correlation between rRNA content and toluene degradation is valid only if toluene is the limiting substrate. During the operation of the biofilter, toluene vapor was generated by bubbling air through liquid toluene with a high volumetric flow, suggesting that oxygen was supplied in ample amounts. Furthermore, a nutrient salt solution was continuously added in surplus after the initial discovery that the nutrient salts concentrations seemed to be limiting (data not shown). Thus, the supply of carbon was considered to be limiting in this system.

The approach presented here illustrates how a description of the physiological state of a subpopulation in a biofilm community may give an indication of how this population is performing in the community. Prediction of substrate concentrations within biofilms requires knowledge of diffusion coefficients, which can be variable in heterogeneous biofilms (24). In the present study, the activity was calculated as a population average, but by applying the spatial resolution of SCLM it may be possible to relate structural complexity to the description of the cellular physiological state. Presently, in situ information about the toluene-degrading population is being incorporated into modeling of the early growth phase of the biofilm, and the reduced activity of the *P. putida* population seems to be necessary to explain biofilm growth and toluene removal kinetics (31a).

ACKNOWLEDGMENTS

This work was supported by the Danish Technical Research Council.
Palle Hobolth, Hobolth DNA Syntese (Hillerød, Denmark), is acknowledged for sequencing of the 16S rRNA. Doug Caldwell is acknowledged for pointing out the possibilities of three-dimensional visualization with the Spyglass software.

REFERENCES

1. **Amann, R. I., L. Krumholz, and D. A. Stahl.** 1990. Fluorescent-oligonucleotide probing of whole cells for determinative, phylogenetic, and environmental studies in microbiology. J. Bacteriol. **172:**762–770.
2. **Amann, R. I., W. Ludwig, and K. H. Schleifer.** 1995. Phylogenetic identification and in situ detection of individual microbial cells without cultivation. Microbiol. Rev. **59:**143–169.
3. **Amann, R. I., J. Stromley, R. Devereux, R. Key, and D. A. Stahl.** 1992. Molecular and microscopic identification of sulfate-reducing bacteria in multispecies biofilms. Appl. Environ. Microbiol. **58:**614–623.
4. **Bertani, G.** 1951. Studies on lysogenesis. I. The mode of phage liberation by lysogenic *Escherichia coli*. J. Bacteriol. **62:**293–300.
5. **Bloem, J., D. K. van Mullen, and P. R. Bolhuis.** 1992. Microscopic counting and calculation of species abundances and statistics in real time with an MS-DOS personal computer, applied to bacteria in soil smears. J. Microbiol. Methods **16:**203–213.
6. **Bremer, H., and P. P. Dennis.** 1987. Modulation of chemical composition and other parameters of the cell cycle by growth rate, p. 1527–1542. *In* F. C. Neidhardt, J. L. Ingraham, K. B. Low, B. Magasanik, M. Schaechter, and H. E. Umbarger (ed.), *Escherichia coli* and *Salmonella typhimurium*: cellular and molecular biology. American Society for Microbiology, Washington, D.C.
7. **Broholm, K., B. K. Jensen, T. H. Christensen, and L. Olsen.** 1990. Toxicity of 1,1,1-trichloroethane and trichloroethene on a mixed culture of methane-oxidizing bacteria. Appl. Environ. Microbiol. **56:**2488–2493.
8. **Brosius, J., T. J. Dull, D. D. Sleeter, and H. F. Noller.** 1981. Gene organization and primary structure of a ribosomal RNA operon from *Escherichia coli*. J. Mol. Biol. **148:**107–127.
9. **Caldwell, D. E., D. R. Korber, and J. R. Lawrence.** 1992. Imaging of bacterial cells by fluorescence exclusion using scanning confocal laser microscopy. J. Microbiol. Methods **15:**249–261.
10. **Clark, J. D., and O. Maaløe.** 1967. DNA replication and the cell cycle in *Escherichia coli* cells. J. Mol. Biol. **23:**99–112.
11. **Costerton, J. W., A. Lewandowski, D. DeBeer, D. E. Caldwell, D. R. Korber, and G. James.** 1994. Biofilms, the customized microniche. J. Bacteriol. **176:** 2137–2142.
12. **DeBeer, D., P. Stoodley, F. Roe, and Z. Lewandowski.** 1994. Effects of biofilm structure on oxygen distribution and mass transport. Biotechnol. Bioeng. **43:**1131–1138.
13. **de Lorenzo, V., E. Linsay, B. Kessler, and K. T. Timmis.** 1993. Analysis of *Pseudomonas* gene products using *lacI^{q}Ptrp-lac* plasmids and transposons that confer conditional phenotypes. Gene **123:**17–24.
14. **Dubois, M., K. A. Gilles, J. K. Hamilton, P. A. Rebers, and F. Smith.** 1956.

Colorimetric method for determination of sugar and related substances. Anal. Chem. **28:**350–355.
15. **Felsenstein, J.** 1993. PHYLIP (phylogeny inference package) version 3.5c. Department of Genetics, University of Washington, Seattle.
16. **Gottschal, J. C., and L. Dijkhuizen.** 1988. The place of the continuous culture in ecological research, p. 19–49. *In* J. W. T. Wimpenny (ed.), CRC handbook of laboratory model systems for microbial ecosystems. CRC Press, Inc., Boca Raton, Fla.
17. **Harremoës, P.** 1978. Biofilm kinetics, p. 82–109. *In* R. Mitchell (ed.), Water pollution microbiology. John Wiley, New York.
18. **Jensen, K. F., and S. Pedersen.** 1990. Metabolic growth rate control in *Escherichia coli* may be a consequence of subsaturation of the macromolecular biosynthetic apparatus with substrates and catalytic components. Microbiol. Rev. **54:**89–100.
19. **Kinniment, S. L., and J. W. T. Wimpenny.** 1992. Measurements of the distribution of adenylate concentrations and adenylate energy charge across *Pseudomonas aeruginosa* biofilms. Appl. Environ. Microbiol. **58:**1629–1635.
20. **Korber, D. R., G. James, and J. W. Costerton.** 1994. Evaluation of fleroxacin activity against established *Pseudomonas fluorescens* biofilms. Appl. Environ. Microbiol. **60:**1663–1669.
21. **Krogfelt, K. A., L. K. Poulsen, and S. Molin.** 1993. Identification of coccoid *Escherichia coli* BJ4 cells in the large intestine of streptomycin-treated mice. Infect. Immun. **61:**5029–5034.
22. **Lauritsen, F. R.** 1990. A new membrane inlet for on-line monitoring of dissolved volatile organic compounds with mass spectrometry. Int. J. Mass Spectrometry Ion Processes **95:**259–268.
23. **Lawrence, J. R., D. R. Korber, B. D. Hoyle, J. W. Costerton, and D. E. Caldwell.** 1991. Optical sectioning of microbial biofilms. J. Bacteriol. **173:** 6558–6567.
24. **Lawrence, J. R., G. M. Wolfaardt, and D. R. Korber.** 1994. Determination of diffusion coefficients in biofilms by confocal laser microscopy. Appl. Environ. Microbiol. **60:**1166–1173.
25. **Lowry, O. H., N. J. Rosebrough, A. L. Farr, and R. J. Randall.** 1951. Protein measurement with the Folin phenol reagent. J. Biol. Chem. **193:**265–275.
26. **Maidak, B. L., N. Larsen, M. J. McCaughey, R. Overbeek, G. J. Olsen, K. Fogel, J. Blandy, and C. R. Woese.** 1994. The ribosomal database project. Nucleic Acids. Res. **22:**3485–3487.
27. **Marqués, S., and J. L. Ramos.** 1993. Transcriptional control of the *Pseudomonas putida* TOL plasmid catabolic pathway. Mol. Microbiol. **9:**923–929.
28. **Massol-Deyá, A. A., J. Whallon, R. F. Hickey, and J. M. Tiedje.** 1995. Channel structures in aerobic biofilms of fixed-film reactors treating contaminated groundwater. Appl. Environ. Microbiol. **61:**769–777.
29. **Møller, S., C. S. Kristensen, L. K. Poulsen, J. M. Carstensen, and S. Molin.** 1995. Bacterial growth on surfaces: automated image analysis for quantification of growth rate-related parameters. Appl. Environ. Microbiol. **61:**741–748.
29a. **Nielsen, A. T.** Personal communication.
30. **Pang, P., and H. H. Winkler.** 1994. The concentration of stable RNA and ribosomes in *Rickettsia prowazekii*. Mol. Microbiol. **12:**115–120.
31. **Pedersen, A. R., and E. Arvin.** 1995. Removal of toluene in waste gases using a biological trickling filter. Biodegradation **6:**109–118.
31a. **Pedersen, A. R., et al.** Unpublished data.
32. **Pedersen, J. C., and C. S. Jacobsen.** 1993. Fate of *Enterobacter cloacae* JP120 and *Alcaligenes eutrophus* AEO106(pRO101) in soil during water stress: effects on culturability and viability. Appl. Environ. Microbiol. **59:**1560–1564.
33. **Poulsen, L. K., G. Ballard, and D. A. Stahl.** 1993. Use of rRNA fluorescence in situ hybridization for measuring the activity of single cells in young and established biofilms. Appl. Environ. Microbiol. **59:**1354–1360.
34. **Poulsen, L. K., F. Lan, C. S. Kristensen, P. Hobolth, S. Molin, and K. A. Krogsfelt.** 1994. Spatial distribution of *Escherichia coli* in the mouse large intestine inferred from rRNA in situ hybridization. Infect. Immun. **62:**5191–5194.
35. **Ramsing, N. B., M. Kühl, and B. B. Jørgensen.** 1993. Distribution of sulfate-reducing bacteria in a photosynthetic biofilm determined by 16S rRNA binding oligonucleotide probes and microelectrodes. Appl. Environ. Microbiol. **59:**3840–3849.
36. **Raskin, L., L. K. Poulsen, D. R. Noguera, B. E. Rittmann, and D. A. Stahl.** 1994. Quantification of methanogenic groups in anaerobic biological reactors by oligonucleotide probe hybridization. Appl. Environ. Microbiol. **60:** 1241–1248.
37. **Rittmann, B. E., and J. A. Manem.** 1992. Development and experimental evaluation of a steady-state, multispecies biofilm model. Biotechnol. Bioeng. **39:**914–922.
38. **Rittmann, B. E., and P. L. McCarty.** 1980. Model of steady-state biofilm kinetics. Biotechnol. Bioeng. **22:**2343–2357.
39. **Schaechter, M., O. Maaløe, and N. O. Kjeldgaard.** 1958. Dependency on medium and temperature of cell size and chemical composition during balanced growth of *Salmonella typhimurium*. J. Gen. Microbiol. **19:**592–606.
40. **Schleifer, K. H., R. I. Amann, W. Ludwig, C. Rothemund, N. Springer, and D. Dorn.** 1992. Nucleic acid probes for the identification and *in situ* detection of pseudomonads, p. 127–134. *In* E. Galli, S. Silver, and B. Witholt (ed.), *Pseudomonas*: molecular biology and biotechnology. American Society for Microbiology, Washington, D.C.
41. **Stoodley, P., D. DeBeer, and Z. Lewandowski.** 1994. Liquid flow in biofilm systems. Appl. Environ. Microbiol. **60:**2711–2716.
42. **Sørensen, J., J. Skouv, A. Jørgensen, and O. Nybroe.** 1992. Rapid identification of environmental isolates of *Pseudomonas aeruginosa*, *P. fluorescens* and *P. putida* by SDS-PAGE analysis of whole-cell protein patterns. FEMS Microbiol. Ecol. **101:**41–50.
43. **van Overbeek, L. S., J. D. van Elsas, J. T. Trevors, and M. E. Starodub.** 1990. Long-term survival of and plasmid stability in *Pseudomonas* and *Klebsiella* species and appearance of nonculturable cells in agricultural drainage water. Microb. Ecol. **19:**239–249.
44. **Wagner, M., R. I. Amann, P. Kämpfer, B. Assmus, A. Hartmann, P. Hutzler, N. Springer, and K. H. Schleifer.** 1995. Identification and *in situ* detection of gram-negative filamentous bacteria in activated sludge. Syst. Appl. Microbiol. **17:**405–417.
45. **Wagner, M., B. Assmus, A. Hartmann, P. Hutzler, and R. I. Amann.** 1994. *In situ* analysis of microbial consortia in activated sludge using fluorescently labelled, rRNA-targeted oligonucleotide probes and confocal scanning laser microscopy. J. Microsc. **176:**181–187.
46. **Wagner, M., R. Erhart, W. Manz, R. I. Amann, H. Lemmer, D. Wedi, and K. H. Schleifer.** 1994. Development of an rRNA-targeted oligonucleotide probe specific for the genus *Acinetobacter* and its application for in situ monitoring in activated sludge. Appl. Environ. Microbiol. **60:**792–800.